Supramolecular Chemistry
Publication details, including instructions for authors and subscription information:
http://www.informaworld.com/smpp/title~content=t713649759

Calixarene-stabilised cobalt nanoparticle rings: Self-assembly and collective magnetic properties

Alexander Wei[a]; Steven L. Tripp[a]; Jie Liu[a]; Takeshi Kasama[bc]; Rafal E. Dunin-Borkowski[d]
[a] Department of Chemistry and The Birck Nanotechnology Centre, Purdue University, West Lafayette, IN, USA [b] Frontier Research System, Institute of Chemical and Physical Research, Hatoyama, Japan [c] Department of Materials Science and Metallurgy, University of Cambridge, Cambridge, United Kingdom [d] Centre for Electron Nanoscopy, Technical University of Denmark, Lyngby, Denmark

To cite this Article Wei, Alexander , Tripp, Steven L. , Liu, Jie , Kasama, Takeshi and Dunin-Borkowski, Rafal E.(2009) 'Calixarene-stabilised cobalt nanoparticle rings: Self-assembly and collective magnetic properties', Supramolecular Chemistry, 21: 3, 189 — 195
To link to this Article: DOI: 10.1080/10610270802546044
URL: http://dx.doi.org/10.1080/10610270802546044

Supramolecular Chemistry
Vol. 21, Nos. 3–4, April–June 2009, 189–195

Taylor & Francis
Taylor & Francis Group

Calixarene-stabilised cobalt nanoparticle rings: Self-assembly and collective magnetic properties

Alexander Wei[a]*, Steven L. Tripp[a], Jie Liu[a], Takeshi Kasama[b,c] and Rafal E. Dunin-Borkowski[d]

[a]*Department of Chemistry and The Birck Nanotechnology Centre, Purdue University, West Lafayette, IN, USA;* [b]*Frontier Research System, Institute of Chemical and Physical Research, Hatoyama, Japan;* [c]*Department of Materials Science and Metallurgy, University of Cambridge, Cambridge, United Kingdom;* [d]*Centre for Electron Nanoscopy, Technical University of Denmark, Lyngby, Denmark*

(*Received 22 June 2008; final version received 10 October 2008*)

Calixarenes can be used to promote the self-assembly of thermoremanent cobalt nanoparticles into bracelet-like rings below 100 nm in diameter. These kinetically stable assemblies are regulated by the equilibrium between enthalpic gain (dipole–dipole and long-range van der Waals interactions) and entropic loss, analogous to the thermodynamic balance of forces governing supramolecular self-assembly. Examination of the Co nanoparticle rings by electron holography (an electron microscopy technique for imaging in-plane magnetic induction) reveals the existence of chiral flux closure (FC) domains at room temperature, comprising a 'racemic' mixture of clockwise and anticlockwise states. Furthermore, these FC polarisations can be reversed by applying out-of-plane magnetic pulses (H_z) in alternating directions. This switching behaviour has no known analogy at the macroscopic level, and may represent a uniquely nanoscale phenomenon.

Keywords: calixarenes; encapsulation; magnetism; nanoparticles; self-assembly; transmission electron microscopy

Introduction

Annular magnetic nanostructures have intriguing potential as non-volatile memory elements and for high-density information storage (*1*). Magnetic rings are well known to support bistable, vortex-like domains known as flux closure (FC), and can be used as binary data elements with minimal crosstalk between bits, permitting their 2D or 3D organisation into densely packed structures. This strategy was used many years ago using ferrite memory cores for data registry (*2*, *3*), prior to the advent of semiconductor-based devices. More recently, magnetic rings have been investigated as switches for non-volatile random-access memory (NVRAM) and other magnetoelectronic applications. These are being pursued with the prospects of achieving ultradense information storage by reducing bit size to nanometre length scales, limited ultimately by the single-domain limit as determined by the magnetocrystalline anisotropy of the host material (*4*).

Many methods for producing magnetic nanostructures with rationally designed features involve 'top-down' lithographic approaches, but the reproducible fabrication of nanosized features below 100 nm can be very challenging (*5*). On the other hand, magnetic nanoparticles of different shapes, sizes and compositions are now readily accessible by chemical synthesis and may be organised into higher order structures, including rings (*6–8*). Self-assembly continues to have enormous potential for engineering nanostructures with spatial control at molecular length scales: recent efforts in nanoparticle self-assembly have focused on increasing control over the dimensionality [e.g. 1D nanostructures (*9*) and the formation of binary superlattices (*10*)] and on the interparticle spacing between elements. In the case of magnetic nanoparticle assemblies, these parameters have a strong influence on the dipolar and exchange coupling between particles, giving rise to collective magnetic properties that are both novel and tunable (*11*). For instance, magnetisation studies on films of ligand-stabilised nanoparticles comprised of Co or FePt have indicated a strong correlation between blocking temperatures and spacing-dependent interparticle coupling (*12–14*). Ordered 2D arrays of Co or Fe nanoparticles have also been shown to support highly correlated states (superferromagnetism) at low temperatures (*15*, *16*), with higher order effects being manifest even at room temperature (*17*).

Here we summarise some recent studies on the self-assembly and collective properties of Co nanoparticle rings, with an emphasis on magnetic FC states and a recently disclosed switching phenomenon triggered by coaxial magnetic fields (*18*). The Co nanoparticles are dispersed using *C*-undecylcalix[4]resorcinarene (**1**), whose macrocyclic headgroup is well matched for nanoparticle encapsulation and whose splayed hydrocarbon chains endow colloidal nanoparticles with superior dispersion stability in organic solvents (Figure 1(a)) (*6*, *19*). The FC states are characterised by off-axis electron holography (EH), a specialised electron microscopy technique that can image magnetic induction with

*Corresponding author. Email: alexwei@purdue.edu

ISSN 1061-0278 print/ISSN 1029-0478 online

DOI: 10.1080/10610270802546044
http://www.informaworld.com

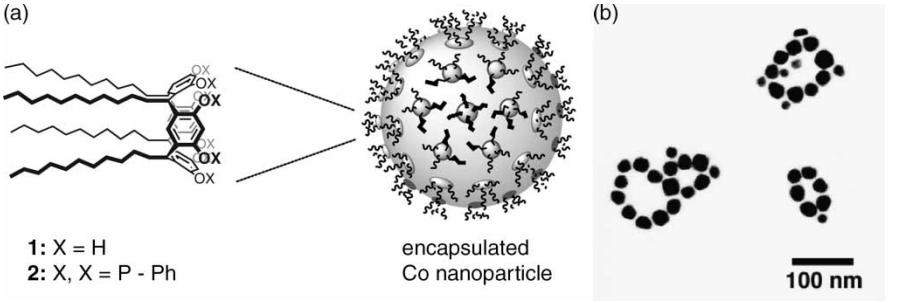

Figure 1. (a) Co nanoparticles stabilised by *C*-undecylcalix[4]resorcinarene **1**. Polycrystalline Co nanoparticles were prepared by the thermolysis of $Co_2(CO)_8$ in the presence of tetraphosphonite **2**. (b) TEM image (Philips EM-400, 80 kV) of bracelet-like Co nanoparticle rings, deposited on a carbon-coated grid from a toluene dispersion and dried in air. Reprinted in part from Ref. (*6a*) with permission (©2002 American Chemical Society).

nanometre spatial resolution (*20*). Both the FC states and the switching mechanism are remarkably robust with respect to ring size and geometry. By understanding the factors that contribute towards nanoparticle ring self-assembly and the FC switching process, one may identify opportunities to apply supramolecular principles for assembling magnetic nanomaterials into higher order structures with technologically useful properties.

Results and discussion

Self-assembly of magnetic nanoparticle rings

Several methods are available for directing the assembly of superparamagnetic nanoparticles. External magnetic fields have been widely applied towards 1D chain assembly (*21*), but can also be used to organise superparamagnetic particles into 2D arrays (*22*). Magneto-hydrodynamic effects in ferrofluids can also produce mesoscopic islands with a variety of 3D topologies as a function of the applied field (*23*). With respect to ring formation, surface force gradients under non-equilibrium conditions, such as those produced during solvent evaporation and surface dewetting, can deposit magnetic nanoparticles into micron or submicron ring-shaped assemblies (*8*).

Weakly ferromagnetic (thermoremanent) nanoparticles are capable of dipole-directed assembly, and can spontaneously assemble into rings of discrete particle count (*6*, *7*) as well as chains of various length (*24*, *25*). Magnetic nanoparticle rings have a lower net dipole than chains (the magnetostatic energy of the FC state is zero), so their formation should be favoured when dispersion conditions are optimised for their self-assembly into clusters with low particle count. Molecular dynamics simulations on discrete ensembles of dipolar particles ($N < 10$) confirm a marked preference for forming rings rather than chains at zero field (*26*). In the absence of externally applied forces, the relative distribution between ring and chain self-assembly is determined by the balance of enthalpic interactions (namely magnetic dipolar couplings, which vary as a function of $1/r^3$) and entropic factors, and can be manipulated by adjusting particle concentrations and dispersion conditions (*6*). Additional factors such as particle shape, the strength of non-directional van der Waals interactions and entropic steric repulsion also come into play. However, rings can be disrupted by applied magnetic fields, as the dipoles of individual particles will attempt to align with the external field lines and destabilise the collective FC state (*6a*).

We have investigated the self-assembly of magnetic nanoparticle rings from thermoremanent, single-domain Co nanoparticles ($d = 27 \pm 4$ nm), using calixarene **1** as a dispersing surfactant in nonpolar solvents (Figure 1) (*6*, *18*, *19*). Calixarene-encapsulated Co nanoparticles have been shown to spontaneously assemble into bracelet-like rings with discrete particle count, and deposited as such onto carbon-coated substrates for the analysis by transmission electron microscopy (TEM). Subnanomolar concentrations of polycrystalline Co nanoparticles ($d = 27 \pm 4$ nm; *ca.* 10^{13} particles/mL) were initially dispersed in millimolar concentrations of **1**, resulting in a significant population of rings containing 5–10 particles (*6a*). The median ring size could be reduced by diluting the dispersion prior to deposition, increasing the population of five- and six-membered rings with overall diameters below 100 nm (*6b*). Smaller Co nanoparticles ($d < 15$ nm) with superparamagnetic character at room temperature were not directly involved in dipole-directed self-assembly, and were generally only incorporated as satellites along the perimeters of the nanoparticle rings.

Calixarene **1** was essential for stabilising the Co nanoparticle rings against drying effects during TEM sample preparation (*6*). Co nanoparticles deposited from toluene solutions with minimal surfactant produced only densely packed particle films, whose formation was driven by non-directional dispersion forces. Increasing the amount of **1** produced a more viscous wetting layer,

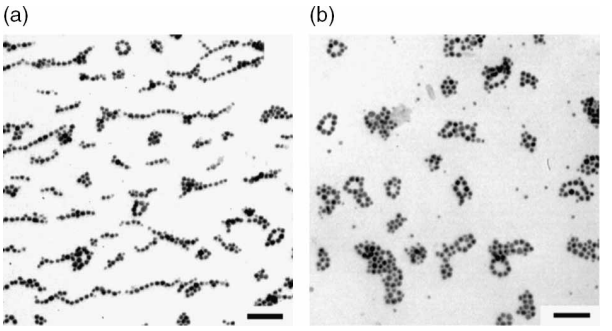

Figure 2. (a) TEM image (Philips EM-400, 80 kV) of Co nanoparticle rings and chains, deposited under the influence of a magnetic field ($B = 225$ G) (*6*). (b) Samples prepared 1 week after prior exposure to a magnetic field resulted in the exclusive appearance of rings. Bar = 200 nm. Reprinted in part from Ref. (*6a*) with permission (©2002 American Chemical Society).

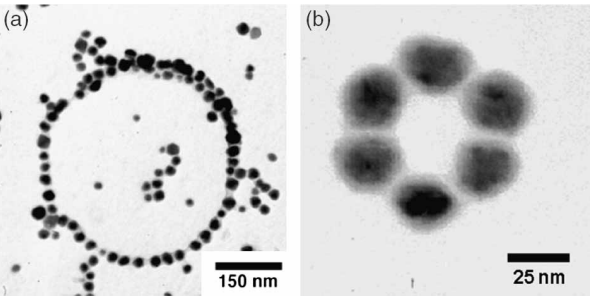

Figure 3. (a) Submicron-sized Co nanoparticle ring formed under dissipative conditions, by deposition from a CH_2Cl_2 dispersion containing **1**. The ring is radially symmetric, but the nanoparticles are unevenly spaced. Reprinted in part from Ref. (*6a*) with permission (©2002 American Chemical Society). (b) Co nanoparticle ring formed by spontaneous, dipole-directed self assembly, by deposition from a toluene dispersion. The six-membered ring is less than 100 nm in diameter.

effectively immobilising the Co nanoparticle rings at an early stage of the drying process. With respect to the mechanism of ring self-assembly, the role of magnetic dipolar interactions was confirmed by applying an in-plane magnetic field during sample preparation, which induced a transition to oriented nanoparticle chains (Figure 2). Removing the field prior to TEM sample preparation resulted in the reappearance of rings, demonstrating that their self-assembly is indeed thermodynamically favoured over that of chains.

Several other mechanisms exist for depositing nanoparticles into annular assemblies, but these produce microrings that are one to two orders of magnitude larger than the bracelet-like nanorings formed by dipole-directed assembly (*8*). Microrings are formed by kinetic processes driven by solvent evaporation, such as hole nucleation in unstable wetting layers (*27*), cell wall formation by Rayleigh–Bénard convection (*8b*), 'breath figures' created by the condensation of water droplets on the rapidly cooling wetting layer (*28*) and contact line pinning during surface dewetting (*29*). In our studies, replacing toluene with the more volatile CH_2Cl_2 provided dissipative conditions that could override the magnetic dipolar interactions, enabling the formation of Co microrings with high radial symmetry (Figure 3) (*6a*). However, a close inspection of such rings revealed numerous gaps between particles, whereas the nanoparticle rings formed by dipole-directed assembly were consistently in close contact. The latter structures indicate that the Co nanoparticles experience maximum dipolar coupling, which can be expected to reinforce the thermoremanent stability of their magnetic FC states.

TEM and EH studies

Co nanoparticle rings formed by dipole-directed self-assembly were deposited onto Cu grids coated with holey carbon films and examined by energy-filtered TEM (also known as electron energy-loss spectroscopy), a chemical imaging technique with nanometre resolution (*30*). The elemental distribution maps of Co, O and C correlate, respectively, with a core of pure Co, a 3–4 nm thick shell of CoO and a supporting layer of calixarene **1** (Figure 4). The in-plane magnetisation of the nanoparticle rings were then characterised at room temperature using EH, which revealed a continuous loop of magnetic induction in accord with the magnetostatic description of the FC state. EH is also phase-sensitive, and can record flux polarisation as clockwise (CW) and anticlockwise (CCW) states. Our studies indicate that the FC states of Co nanoparticle rings are remarkably stable at room temperature, which augurs well for applications in magnetic or magnetoelectronic information storage (*6*, *18*).

EH analysis indicates that every Co nanoparticle ring has an FC state with well-defined polarisation (CW or CCW), despite variations in size and overall structure (Figure 5). Extension of this analysis over a range of samples indicates that CW and CCW polarisations exist as a 'racemic' mixture within the ensemble of self-assembled nanostructures (*6b*). In most cases, the magnetic induction is essentially confined within the ring, with minimal stray flux either inside or outside the self-assembled nanostructure. The continuity of the magnetostatic FC state is not disrupted by deviations from radial symmetry or by grain boundaries within particles, although the latter may introduce some sharp transitions in magnetisation direction. Rings with outcropping (exocyclic) nanoparticles also support polarised FC states, although these protuberances can cause the magnetic flux to diverge and stray well beyond the physical perimeter of the ring (e.g. Figure 5(f)). FC states are also supported by other types of self-assembled Co nanostructures, which are currently under investigation.

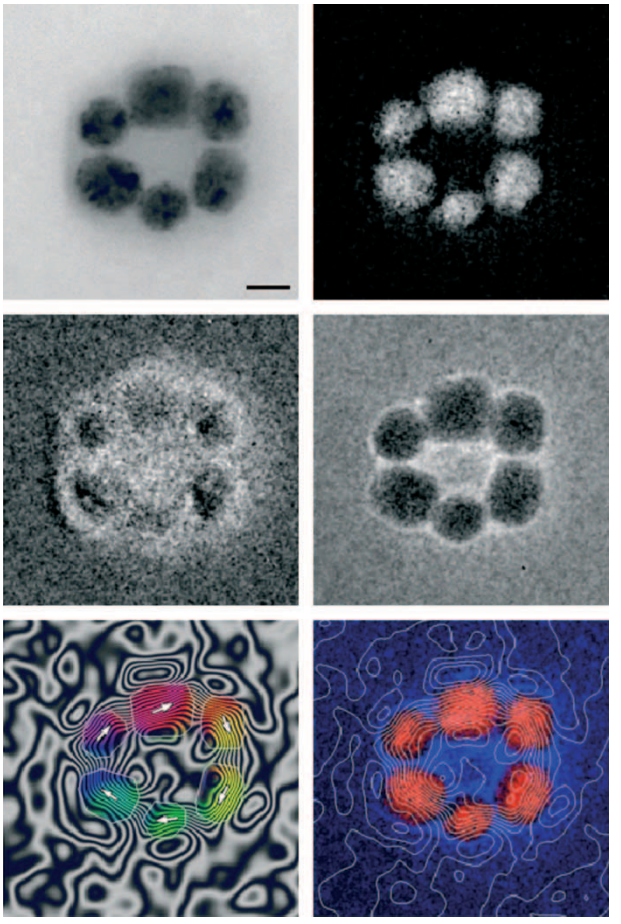

Figure 4. Energy-filtered TEM images of six-membered Co nanoparticle ring. Upper left, bright-field zero-loss image (scale bar = 20 nm); upper right, Co elemental map; middle left, O elemental map; middle right, C elemental map; lower left, EH of magnetic induction acquired at room temperature, with FC (CW) polarisation indicated by white arrows; lower right, EH superimposed on Co elemental map (lightly shaded). Magnetic flux enclosed between adjacent contours is $h/128e$; the linewidth is inversely proportional to the in-plane magnetic induction, providing a measure of its strength.

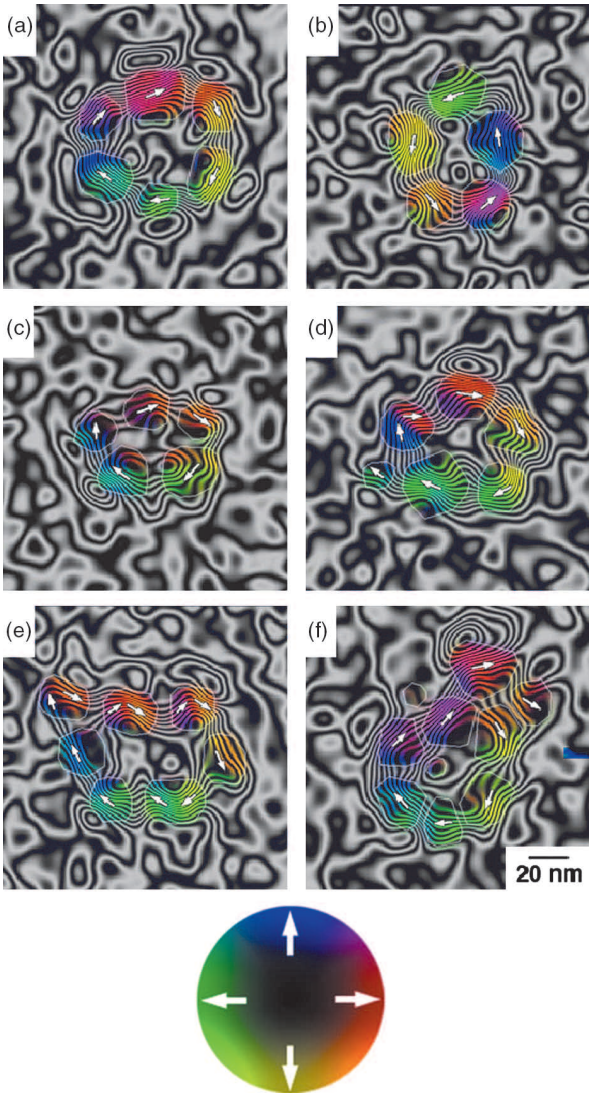

Figure 5. (a–f) EH images of in-plane magnetic induction within various Co nanoparticle rings. The direction of magnetic induction within the ferromagnetic Co cores are colour-coded (colour wheel legend at bottom); the net magnetisation of each domain is indicated by a white arrow. Magnetic flux enclosed between adjacent contours is $h/128e$; contour spacing is 0.049 rads.

FC reversal by out-of-plane magnetic fields

The Co nanoparticle rings have the remarkable ability to reverse their in-plane FC polarisations upon a brief exposure to a coaxial (H_z) magnetic field (*18*). This phenomenon is counter-intuitive, as a strong H_z field could effectively erase the memory of the previous magnetic state; nevertheless, the restored FC state is strongly correlated with prior FC polarisation (Figure 6). An important point to make is that the starting FC states are already synchronised with exposure to a coaxial magnetic field ($H_z = 2$ T, defined as the $+H_z$ direction). This initial exposure is a consequence of routine electron-beam focusing, prior to EH analysis at zero field. While this might first appear to have little effect on FC polarisations (a mixture of CW and CCW states is typically observed), the initial $+H_z$ exposure can determine the response of individual FC states to subsequent coaxial magnetic pulses.

Co nanoparticle rings (following the initial +2-T exposure) were subjected to magnetic pulses in the $+H_z$ or $-H_z$ direction by manipulating the TEM objective lens current and its relation to the ring axis (*18*), then analysed by EH at zero field to examine their effects on FC polarisation. The Co nanoparticle rings displayed a remarkable level of retention when exposed to magnetic pulses in the $+H_z$ direction: in the six-membered ring shown below, the FC state did not switch or scramble with

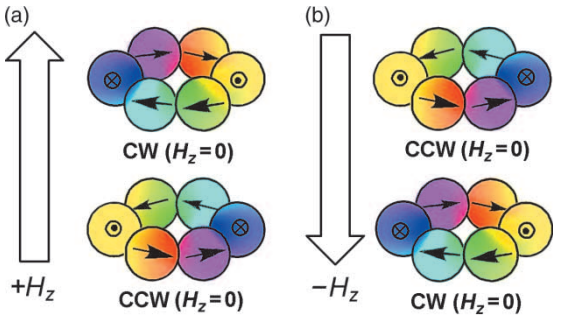

Figure 6. H_z-induced FC reversal in individual Co nanoparticle rings (*18*). (a) Clockwise (CW) and anticlockwise (CCW) FC states are imaged by EH under zero-field conditions, with prior exposure to a coaxial magnetic field ($H_z = +2$ T) during electron-beam focusing. (b) The polarisation of the FC states can be switched by applying an H_z pulse in the $-z$ direction. Reprinted with permission from Wiley-VCH Verlag GmbH.

consecutive application of $+H_z$ fields as strong as 2 T, although minor perturbations in magnetic flux and the direction of individual nanoparticle dipole moments could be observed (Figure 7(a) and (b)). The FC state was also essentially unperturbed by the application of out-of-plane magnetic pulses with in-plane ($H_{x,y}$) magnetisation as high as 0.5 T; again, only minor changes in magnetic flux were observed (Figure 7(c)).

On the other hand, the FC polarisation could be switched by exposure to a $-H_z$ pulse on the order of 1600 Oe (Figure 7(d)). Again, the switched FC state did not experience further changes in polarisation if magnetic pulses were consecutively delivered in the $-H_z$ direction, whereas applying H_z in alternating directions produced multiple FC reversals (Figure 8) (*18*). Additional EH analyses on a series of polycrystalline and single-crystal Co nanoparticle rings have established that (i) the H_z-induced FC reversal is quite general, much like the FC state itself and (ii) the threshold for H_z-induced FC switching (coercivity) is increased by the higher magnetocrystalline anisotropy and dipolar coupling between nanoparticles (*18*). Overall, these studies demonstrate that alternating H_z pulses can provide an effective mechanism for inverting in-plane FC states, based on the history of prior coaxial magnetisations.

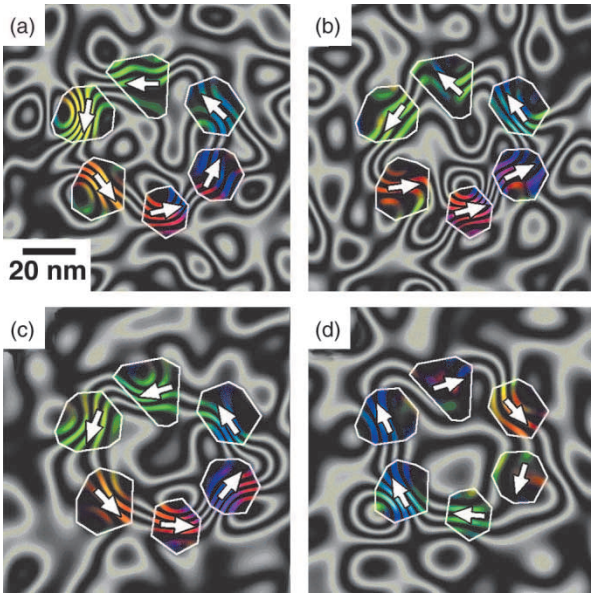

Figure 7. FC polarisations and magnetic induction maps of a six-membered Co nanoparticle ring obtained at zero field, following application of out-of-plane magnetic fields. (a) After initial exposure to out-of-plane field at normal incidence ($H_z = +2$ T); (b) repeat exposure ($H_z = +2$ T); (c) exposure to out-of-plane field at 15° angle of incidence ($H_z = +1.93$ T; $H_{x,y} = 0.52$ T); (d) exposure to inverted magnetic field ($H_z = -1620$ Oe). The contour spacing is 0.098 rads ($h/64e$).

In summary, the encapsulation of thermoremanent Co nanoparticles by calixarene **1** provides dispersion conditions that favour the formation of bracelet-like Co nanoparticle rings less than 100 nm in diameter. The rings are formed by dipole-directed self-assembly, but the dispersion forces are sufficiently weak that they can likely be redirected by supramolecular recognition motifs, providing opportunities to control ring size or to form novel self-assembled nanostructures. EH analysis of Co nanoparticle rings reveal chiral, bistable FC states at room temperature, regardless of variations in their geometry or size. The FC polarisations can be reliably switched by applying coaxial magnetic fields, with a strong correlation to the 'memory' of prior H_z magnetisations. The novel H_z-induced FC switching mechanism has not been previously observed in magnetic

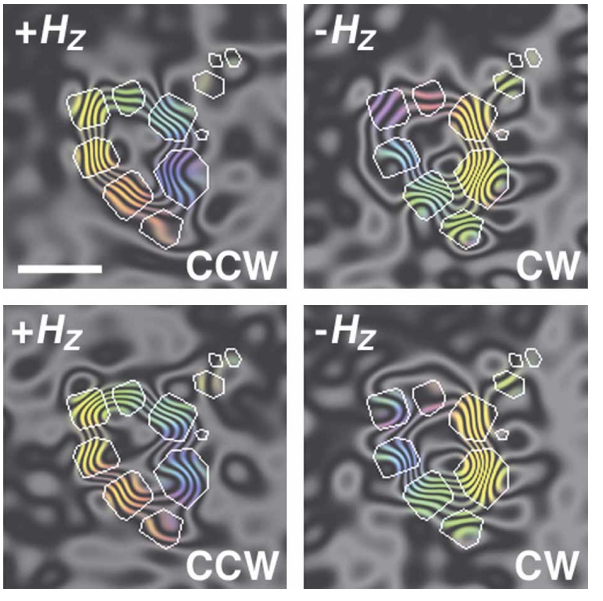

Figure 8. Multiple FC reversals of a seven-membered fcc-Co nanoparticle ring, switched by alternating $+H_z$ and $-H_z$ pulses (from upper left to lower right). The contour spacing is 0.196 rads ($h/32e$); scale bar = 50 nm. Reprinted with permission from Wiley-VCH Verlag GmbH.

microstructures, and may possibly represent a uniquely nanoscale phenomenon. Greater control over nanoparticle self-assembly may open up opportunities for integrating Co nanorings with conductive nanostructures (i.e. nanowires) to create rotaxane nano-heterostructures, as candidate magnetoelectronic components for emerging NVRAM systems.

Materials and methods

Resorcinarene **1** was prepared in a one-step procedure as described by Aoyama and co-workers (*31*), and used in its monohydrate form. Polycrystalline Co nanoparticles were prepared by the thermolysis of $Co_2(CO)_8$ in toluene in the presence of C11 resorcinarene tetraphosphinite **2**, then redispersed and fractionated in the presence of **1** as previously described (*6a*). For dipole-directed self-assembly, Co nanoparticles were dispersed at a concentration of 10^{12} particles/mL in a 1 μM solution of **1** in toluene, and sonicated for 1 h in an ice-cooled ultrasonic cleaning bath. The nanoparticle suspensions were stable at zero field at ambient temperatures over a period of many weeks.

Co nanoparticle suspensions were drop-cast onto carbon-coated copper TEM grids (400 mesh, Electron Microscopy Sciences) for 30 s. The bulk of this suspension was removed by holding an adsorptive tissue to one edge of the grid, and the residual wetting layer was allowed to dry in air without further disturbances. This resulted in the deposition of many Co nanoparticle clusters containing three to eight particles, assembled in various shapes including rings, short chains and close-packed aggregates. The samples were briefly treated with an oxygen plasma prior to TEM analysis.

Off-axis EH and energy-filtered imaging were performed using a Philips CM-300 transmission electron microscope equipped with a Lorentz lens, a rotatable electron biprism (200 V) located in the selected-area aperture plane, and a Gatan multiscan CCD camera (2048 × 2048 pixels). The diffuse oxygen elemental map (slightly misaligned) is reflective of the plasma cleaning prior to TEM analysis. Nanoparticle assemblies were first exposed to a (+)2-T out-of-plane magnetic field as a consequence of TEM imaging under standard conditions, but kept under field-free conditions at room temperature prior to EH analysis. Thermoremanent states were imaged under zero-field conditions and displayed in the form of contours, with local flux polarisations indicated by a colour wheel and net magnetic moments per particle indicated by white arrows. The holographic interference fringe spacing is 3 nm with a contrast of 25%. The magnetic contribution to the measured holographic phase shift was separated from the mean inner potential contribution by taking the difference between phase images recorded with the sample turned over. The divergent magnetic contours beyond the Co nanoparticle rings (grey areas) are due to statistical noise and/or imperfect subtraction of the mean inner potential contribution of the carbon support film.

Acknowledgements

We gratefully acknowledge the National Science Foundation (CHE-0243496), the Defense Advanced Research Project Agency and the Royal Society for financial support.

References

(1) Zhu, J.-G.; Zheng, Y.; Prinz, G.A. *J. Appl. Phys.* **2000**, *87*, 6668–6673.
(2) Griefer, A.P. *IEEE Trans. Magn.* **1969**, *5*, 774–811.
(3) Russell, L.A.; Whalen, R.M.; Leilich, H.O. *IEEE Trans. Magn.* **1968**, *4*, 134–145.
(4) (a) Weller, D.; Moser, A. *IEEE Trans. Magn.* **1999**, *35*, 4423–4439. (b) Weller, D.; Doerner, M. *Annu. Rev. Mater. Sci.* **2000**, *30*, 611–644.
(5) Heyderman, L.J.; David, C.; Kläui, M.; Vaz, C.A.F.; Rothman, J.; Bland, J.A.C. *J. Appl. Phys.* **2003**, *93*, 10011–10013.
(6) (a) Tripp, S.L.; Pusztay, S.V.; Ribbe, A.E.; Wei, A. *J. Am. Chem. Soc.* **2002**, *124*, 7914–7915. (b) Tripp, S.L.; Dunin-Borkowski, R.E.; Wei, A. *Angew. Chem. Int. Ed.* **2003**, *42*, 5591–5593.
(7) (a) Philipse, A.P.; Maas, D. *Langmuir* **2002**, *18*, 9977–9984. (b) Lee, H.; Purdon, A.M.; Chu, V.; Westervelt, R.M. *Nano Lett.* **2004**, *4*, 995–998.
(8) (a) Shafi, K.V.P.M.; Felner, I.; Mastai, Y.; Gedanken, A. *J. Phys. Chem. B* **1999**, *103*, 3358–3360. (b) Maillard, M.; Motte, L.; Pileni, M.P. *Adv. Mater.* **2000**, *13*, 200–204. (c) Zhou, W.L.; He, J.B.; Fang, J.Y.; Huynh, T.A.; Kennedy, T.J.; Stokes, K.L.; O'Connor, C.J. *J. Appl. Phys.* **2003**, *93*, 7340–7342. (d) Govor, L.V.; Bauer, G.H.; Reiter, G.; Shevchenko, E.; Weller, H.; Parisi, J. *Langmuir* **2003**, *19*, 9573–9576. (e) Gu, H.; Xu, B.; Rao, J.; Zheng, R.K.; Zhang, X.X.; Fung, K.K.; Wong, C.Y.C. *J. Appl. Phys.* **2003**, *93*, 7589–7591. (f) Guo, Q.; Teng, X.; Yang, H. *Nano Lett.* **2004**, *4*, 1657–1662. (g) Liu, Z.; Levicky, R. *Nanotechnology* **2004**, *15*, 1483–1488.
(9) Tang, Z.Y.; Kotov, N.A. *Adv. Mater.* **2005**, *17*, 951–962.
(10) (a) Kiely, C.J.; Fink, J.; Brust, M.; Bethell, D.; Schiffrin, D.J. *Nature* **1998**, *396*, 444–446. (b) Shevchenko, E.; Talapin, D.V.; Kotov, N.A.; O'Brien, S.; Murray, C.B. *Nature* **2006**, *439*, 55–59.
(11) Frankamp, B.L.; Boal, A.K.; Tuominen, M.T.; Rotello, V.M. *J. Am. Chem. Soc.* **2005**, *127*, 9731–9735.
(12) Sun, S.H.; Murray, C.B. *J. Appl. Phys.* **1999**, *85*, 4325–4330.
(13) Petit, C.; Taleb, A.; Pileni, M.P. *J. Phys. Chem. B* **1999**, *103*, 1805–1810.
(14) Sun, S.H.; Murray, C.B.; Weller, D.; Folks, L.; Moser, A. *Science* **2000**, *287*, 1989–1992.
(15) Puntes, V.F.; Krishnan, K.M.; Alivisatos, A.P. *Appl. Phys. Lett.* **2001**, *78*, 2187–2189.
(16) Farrell, D.; Yamamuro, S.; Majetich, S.A. *MRS Symp. Proc.* **2001**, *Spring 2001*, U4.4.
(17) (a) Yamamuro, S.; Farrell, D.; Humfeld, K.D.; Majetich, S.A. *MRS Symp. Proc.* **2001**, *636*, D10.18.11–16. (b) Yamamuro, S.; Farrell, D.F.; Majetich, S.A. *Phys. Rev. B* **2002**, *65*, 224431.

(18) Kasama, T.; Dunin-Borkowski, R.E.; Scheinfein, M.R.; Tripp, S.L.; Liu, J.; Wei, A. *Adv. Mater.* **2008**, *20*, in press (doi: 10.1002/adma.200702941).
(19) (a) Wei, A.; Kim, B.; Pusztay, S.V.; Tripp, S.L.; Balasubramanian, R. *J. Inclusion Phenom. Macrocyclic Chem.* **2001**, *41*, 83–86. (b) Wei, A. *Chem. Commun.* **2006**, 1581–1591.
(20) (a) Dunin-Borkowski, R.E.; McCartney, M.R.; Kardynal, B.; Parkin, S.S.P.; Scheinfein, M.R.; Smith, D.J. *J. Microsc.* **2000**, *200*, 187–205. (b) Dunin-Borkowski, R.E.; Kasama, T.; Wei, A.; Tripp, S.L.; Hytch, M.J.; Snoeck, E.; Harrison, R.J.; Putnis, A. *Microsc. Res. Tech.* **2004**, *64*, 390–402. (c) Thomas, J.M.; Simpson, E.T.; Kasama, T.; Dunin-Borkowski, R.E. *Acc. Chem. Res.* **2008**, *41*, 665–674.
(21) (a) Niu, H.; Chen, Q.; Zhu, H.; Lin, Y.; Zhang, X. *J. Mater. Chem.* **2003**, *13*, 1803–1805. (b) Cheng, G.; Romero, D.; Fraser, G.T.; Hight Walker, A.R. *Langmuir* **2005**, *21*, 12055–12059. (c) Gao, J.; Zhang, B.; Zhang, X.; Xu, B. *Angew. Chem. Int. Ed.* **2006**, *45*, 1220–1223. (d) Keng, P.Y.; Shim, I.; Korth, B.D.; Douglas, J.F.; Pyun, J. *ACS Nano* **2007**, *1*, 279–292.
(22) Giersig, M.; Hilgendorff, M. *J. Phys. D: Appl. Phys.* **1999**, *32*, L111–L113.
(23) (a) Petit, C.; Taleb, A.; Pileni, M.P. *J. Phys. Chem. B* **1999**, *103*, 1805–1810. (b) Legrand, J.; Ngo, A.-T.; Petit, C.; Pileni, M.P. *Adv. Mater.* **2001**, *18*, 53–57. (c) Pileni, M.P. *J. Phys. Chem. B* **2001**, *105*, 3358–3371.
(24) Thomas, J.R. *J. Appl. Phys.* **1966**, *37*, 2914–2915.
(25) Butter, K.; Bomans, P.H.H.; Frederik, P.M.; Vroege, G.J.; Philipse, A.P. *Nature Mater.* **2003**, *2*, 88–91.
(26) Jund, P.; Kim, S.G.; Tománek, D.; Hetherington, J. *Phys. Rev. Lett.* **1995**, *74*, 3049.
(27) (a) Ohara, P.C.; Heath, J.R.; Gelbart, W.M. *Angew. Chem. Int. Ed.* **1997**, *36*, 1078–1080. (b) Ohara, P.C.; Gelbart, W.M. *Langmuir* **1998**, *14*, 3418–3424. (c) Vossmeyer, T.; Chung, S.-W.; Gelbart, W.M.; Heath, J.R. *Adv. Mater.* **1998**, *10*, 351–353.
(28) (a) Gómez-Segura, J.; Kazakova, O.; Davies, J.; Josephs-Franks, P.; Veciana, J.; Ruiz-Molina, D. *Chem. Commun.* **2005**, 5615–5617. (b) Khanal, B.P.; Zubarev, E.R. *Angew. Chem. Int. Ed.* **2007**, *46*, 2195–2198.
(29) (a) Deegan, R.D.; Bakajin, O.; Dupont, T.F.; Huber, G.; Nagel, S.R.; Witten, T.A. *Nature* **1997**, *389*, 827–829. (b) Deegan, R.D. *Phys. Rev. E* **2000**, *61*, 475–485.
(30) Egerton, R.F. *Electron Energy Loss Spectroscopy in the Electron Microscope*; Plenum Press: New York, NY, 1996.
(31) Aoyama, Y.; Tanaka, Y.; Sugahara, S. *J. Am. Chem. Soc.* **1989**, *111*, 5397–5404.